Investigating the relationship between material properties and laser induced damage threshold of dielectric optical coatings at 1064 nm

Riccardo Bassiri*[a], Caspar Clark[b], Iain W. Martin[c], Ashot Markosyan[a], Peter G. Murray[c],
Joseph Tessmer[c], Sheila Rowan[c], Martin M. Fejer[a]

[a]E. L. Ginzton Laboratory, Stanford University, Stanford, California, 94305, USA;
[b]Helia Photonics Ltd., Livingston, EH54 7EJ, UK;
[c]SUPA, School of Physics and Astronomy, University of Glasgow, Glasgow, G12 8QQ, UK

ABSTRACT

The Laser Induced Damage Threshold (LIDT) and material properties of various multi-layer amorphous dielectric optical coatings, including Nb_2O_5, Ta_2O_5, SiO_2, TiO_2, ZrO_2, AlN, SiN, LiF and ZnSe, have been studied. The coatings were produced by ion assisted electron beam and thermal evaporation; and RF and DC magnetron sputtering at Helia Photonics Ltd, Livingston, UK. The coatings were characterized by optical absorption measurements at 1064 nm by Photothermal Common-path Interferometry (PCI). Surface roughness and damage pits were analyzed using atomic force microscopy. LIDT measurements were carried out at 1064 nm, with a pulse duration of 9.6 ns and repetition rate of 100 Hz, in both 1000-on-1 and 1-on-1 regimes. The relationship between optical absorption, LIDT and post-deposition heat-treatment is discussed, along with analysis of the surface morphology of the LIDT damage sites showing both coating and substrate failure.

Keywords: Laser Induced Damage, Photothermal Common-path Interferometry, optical coatings, 1064nm

1. INTRODUCTION

Optical coatings on laser components such as Q-switches and beam-steering elements are subject to intense electric fields and high optical fluences, often capable of destroying absorbing, scattering or mechanically weak thin films. In this study, a series of materials used in everyday processes, were combined to offer a high performance Anti Reflection (AR) coating at 1064 nm. The aim was to identify optimal materials and deposition techniques for high laser damage threshold coatings at 1064 nm, and determine any correlation between measured optical absorption and LIDT.

The coating samples were grown on both sides of well-characterized substrates and measured to ensure an acceptable transmission was achieved. The coatings were then assessed for absorption via the PCI technique yielding valuable information not only about the baseline absorption, but also an absorption profile through and across the surface of each sample. Components from each batch were also assessed for LIDT. Additional samples were also annealed and the effect on optical absorption and LIDT compared.

The Laser Induced Damage Threshold (LIDT) and material properties of various multi-layer amorphous dielectric optical coatings, including Nb_2O_5, Ta_2O_5, SiO_2, TiO_2, ZrO_2, AlN, SiN, LiF and ZnSe, were studied. Here, we present the results of PCI optical absorption, 1000-on-1 and 1-on-1 LIDT measurements, and post-deposition heat-treatment on the coating samples. Atomic Force Microscopy was used in conjunction with optical Nomarski assessment to investigate the extent of laser damage.

2. COATING DEPOSITION TECHNIQUES AND MATERIALS

AR coatings were grown on various deposition systems at Helia Photonics, Scotland, mainly built in-house. The deposition techniques used in this trial were ion assisted electron beam (ebeam) & thermal evaporation, Radio Frequency (RF) and pulsed Direct Current (DC) magnetron sputtering; and thermal only evaporation. An AR coating design was used for all samples and coated on both sides of silica based substrates including Spectrosil 2000, used for PCI absorption and AFM measurement, and Borofloat 33 used for the LIDT measurements. The substrates were ultrasonically cleaned prior to coating to ensure minimal surface contamination. A description of the deposition techniques used and their associated parameters is given in Table 1.

*rbassiri@stanford.edu

Table 1. Deposition techniques and associated parameters

Pumping	Source type	Deposition parameters
Cryo Pump	Ion Assisted [End Hall ~100 eV] reactive electron beam + thermal	100ºC, 1 m source-substrate, start P = 1×10^{-6} mbar, run P = 2.5×10^{-3} mbar
	Pulsed DC (82kHz) reactive sputtering – 4" magnetrons	150ºC, 15 cm source-substrate, start P = 1×10^{-6} mbar, run P = 6×10^{-3} mbar
	RF (13.56MHz) reactive sputtering – 8" magnetrons	50ºC, 20 cm source-substrate, start P = 1×10^{-8} mbar, run P = 8×10^{-3} mbar
Turbo Molecular Pump	Thermal evaporation, non-reactive, Mo boat	200ºC, 35 cm source-substrate, start P = 5×10^{-6} mbar, run P = 3×10^{-4} mbar

Each coating sample had a material composition chosen due to a variety of practical use scenarios, and the target materials and techniques available at the time of deposition. A description of each coating composition and the specific purpose of its investigation is given in Table 2. The transmission measurements are also given and were made with a Perkin Elmer lambda 900 spectrophotometer.

Table 2. Coating material compositions and deposition techniques is given, with measured transmission values and used and purpose of investigation.

#	Coating	T%*	Purpose of investigation
1	//ZrO_2/SiO_2 RF sputter	99.41	Known internal process working well for high power Q-switches.
2	//Ta_2O_5/SiO_2 RF sputter	99.56	Optically low loss materials
3	//Nb_2O_5/SiO_2 RF sputter	97.63	As above but less expensive to grow
4	//TiO_2/SiO_2 ebeam/thermal	99.55	Similar optically to #5, #6 but TiO_2 known to yield rougher films
5	//Nb_2O_5/SiO_2 ebeam/thermal	98.26	As #3 but different technique
6	//Ta_2O_5/SiO_2 ebeam/thermal	99.94	As #2 but different technique
7	//AlN/SiO_2 pDC sputter	98.56	AlN good thermal conductor but pDC SiO_2 known to be 'granular'
8	//AlN/SiN pDC sputter	98.56	As above but SiN as the lower index layer
9	//ZrO_2/SiN pDC sputter	99.52	As a comparison with #1
10	//ZnSe/LiF thermal	99.99	LiF known to be a high laser damage material

* Transmission measured by spectrophotometry @1064nm on Spectrosil 2000

3. PCI OPTICAL ABSORPTION MEASUREMENTS

Optical absorption measurements were made using the PCI technique, which allows the accurate measurement of bulk and coating optical absorption. The PCI technique is based on measuring the thermal lensing caused by the pump beam (CW, $\lambda = 1064$ nm, up to 8 W) and the resulting interference from the phase mismatch between the central and outermost part of the probe beam (CW, $\lambda = 632$ nm, 2.5 mW) [1-3].

Figure 1 shows a schematic of the PCI experimental setup. The detected AC voltage (V_{AC}) signal is comprised of only first-order terms and hence can be normalized to the total probe power (DC output voltage (V_{DC}) of the detector) over that of the independent pump power (W_{pump}), so the value of the absorption loss, α, is simply proportional to the ratio $V_{AC}/V_{DC}/W_{pump}$. The setup was calibrated using a Newport metallic neutral density filter, which had absorption of 22 % at 1064 nm (measured with a Cary 500 spectrophotometer). With these parameters, an optical absorption loss at 1064 nm as low as $\alpha = 0.02$ ppm can be measured using pump powers not higher than 8.0 W.
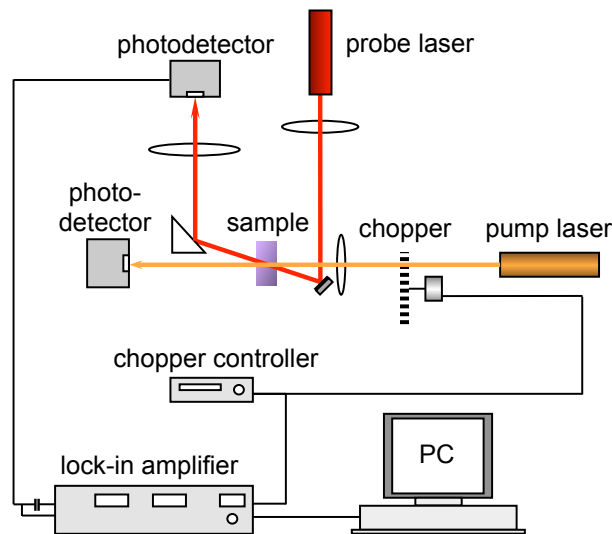
Figure 1. Schematic of the PCI experimental setup.

The recorded signal is read from the crossing point of the pump and probe beams that moves along the pump propagation direction, i.e. perpendicular to the coating in the z-direction (z-scan) or across the coating in the x-direction (x-scan).

In general, in order to ensure the absorption of the coatings is easily distinguishable from the coating, it is preferable to have a substrate with as low absorption as possible when compared to any coating applied to the surface. The absorption of samples of Borofloat 33 and Spectrosil 2000 were studied as candidate substrate materials. Figure 2 shows the z-scans of the substrates, which were 0.25 inches thick. The Borofloat 33 z-scan (figure 2 (a)) shows a large surface absorption likely due to a subsurface polishing imperfection, peaking around 3.3 mm into the scan, and a bulk α = 2200 ppm/cm. Spectrosil 2000 was chosen for samples that underwent PCI absorption measurements due to its low α = 19.5 ppm/cm (figure 2 (b)).
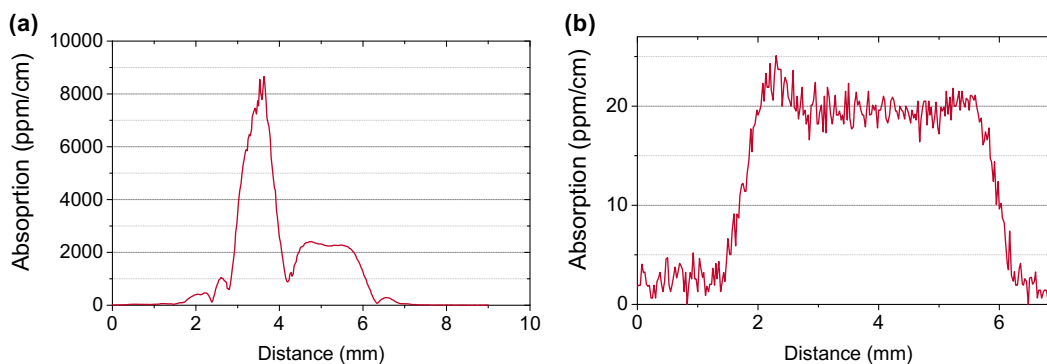

Figure 2. PCI absorption z-scan of the (a) Borofloat 33 and (b) Spectrosil 2000 substrate samples.

For the test coatings, example PCI x-scans highlighting the best and worst coating measurements for the ZrO_2/ SiN and ZrO_2/ SiO_2 coating samples are shown in figure 3. These x-scans probe only the absorption across a 6 mm line on the coating layer. For the ZrO_2/ SiN, figure 3 (a) shows several spikes, with a baseline α = 58 ppm. These spikes may be due to defects such as non-stoichiometric regions, absorbing impurities, and surface contamination; although care is taken to ensure the coating surface is clean and free of any dust during measurement. By comparison, figure 3 (b) shows the ZrO_2/ SiO_2 sample which has a lower baseline α = 9 ppm, and relatively few spikes, indicating a uniform and high quality coating.
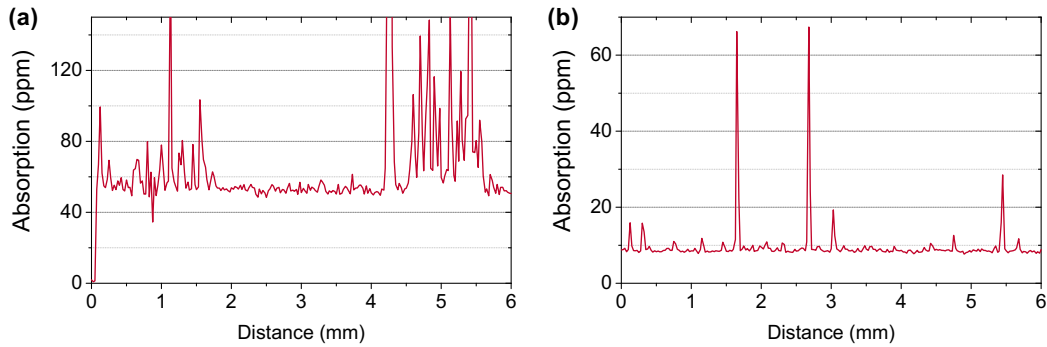
Figure 3. PCI absorption x-scan of the (a) ZrO_2/ SiN and (b) ZrO_2/ SiO_2 coating samples.

The absorption values for all coating samples compared to LIDT measurements will be given in section 5, and were taken from the baseline absorption values measured in the x-scans.

4. LASER INDUCED DAMAGE THRESHOLD

Laser Induced Damage Threshold was assessed at the Lidaris Ltd facility in Vilnius, Lithuania using the first harmonic of pulsed Nd:YAG InnoLas Laser: SpitLight Hybrid laser (λ= 1064 nm, linear polarization, TEM00 single mode, pulse duration 9.6 ± 1 ns), λ /2 plate combined with additional polarizer attenuator, online scattered light damage detection, offline inspection of damage detection using Nomarski microscopy (100 ×). For each sample 411 equally spaced test sites in square grid pattern were used to reduce erratic defect-driven results and assess threshold. The beam diameter in target plane ($1/e^2$) was 203.6 μm.

The coating samples were tested in both 1-on-1 and s-on-1 (s=1000) regimes. Where strong differences between each test regime exists, it is expected that the coating undergoes significant parametric change during the test such as localized anneal or stoichiometric balancing. Figure 4 shows these LIDT results and demonstrates good agreement between these methods.
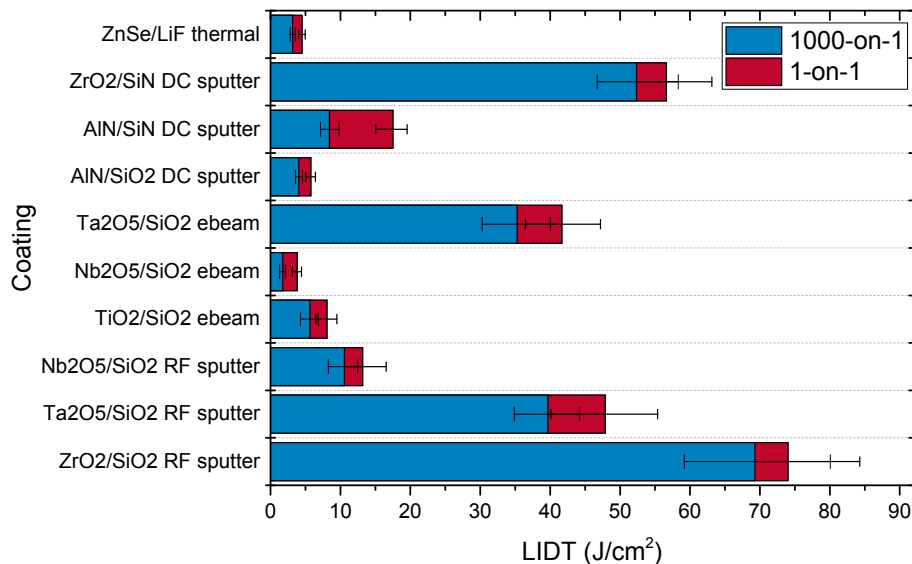

Figure 4. LIDT of coating samples with associated errors, for both 1000-on-1 and 1-on-1 regimes**.**

5. LIDT AND MATERIAL PROPERTIES

The 1-on-1 LIDT measurements compared to the baseline absorption of each coating sample is given in figure 5. The RF sputtered ZrO_2/SiO_2 coating was shown to give the highest damage threshold at 74 J/cm^2 and lowest absorption, $\alpha = 9$ ppm. The lowest damage threshold was measured on the ebeam deposited Nb_2O_5/SiO_2 at 13 J/cm^2 and a relatively high absorption, $\alpha = 45$ ppm.

There does not appear to be a direct correlation between LIDT and optical absorption. This is perhaps not a surprising result given the spread of materials and deposition techniques used. However, when comparing similar coatings between RF sputtering and e-beam deposition techniques, RF sputtering gives both lower absorption and higher LIDT compared with ebeam coatings for both the Ta_2O_5/SiO_2 and Nb_2O_5/SiO_2 samples, as shown with the highlighted green (diagonal stripes) and blue (vertical stripes) measurements in the figure 5.

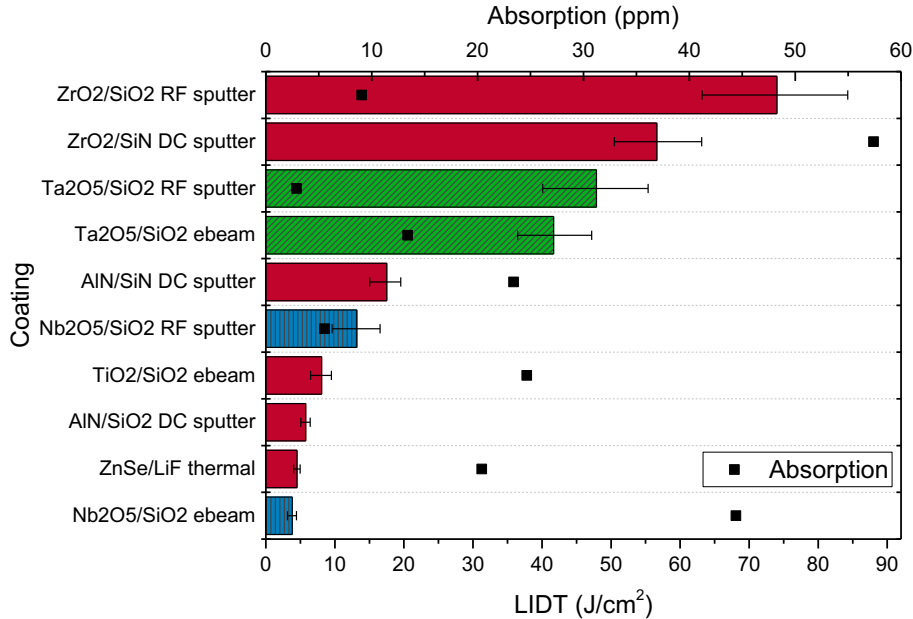

Figure 5. 1-on-1 LIDT compared to baseline PCI absorption, and highlighting differences between RF sputtered ebeam deposition methods for Ta_2O_5/SiO_2 (green, diagonal stripes) and Nb_2O_5/SiO_2 (blue, vertical stripes) samples.

It has been shown that post-deposition annealing of oxide coatings in air can reduce optical absorption [4]. Figure 6 shows the x-scan for the ZrO_2/SiO_2 RF sputtered sample, highlighting the significant improvement in absorption, where an initial $\alpha = 9.1$ ppm for the as-deposited sample was reduced to $\alpha = 2.1$ ppm after annealing at 300°C in air for 24 hrs. There is also a noticeable decrease in the spikes in absorption after annealing, which may indicate that defect sites are also improved with heat-treatment.
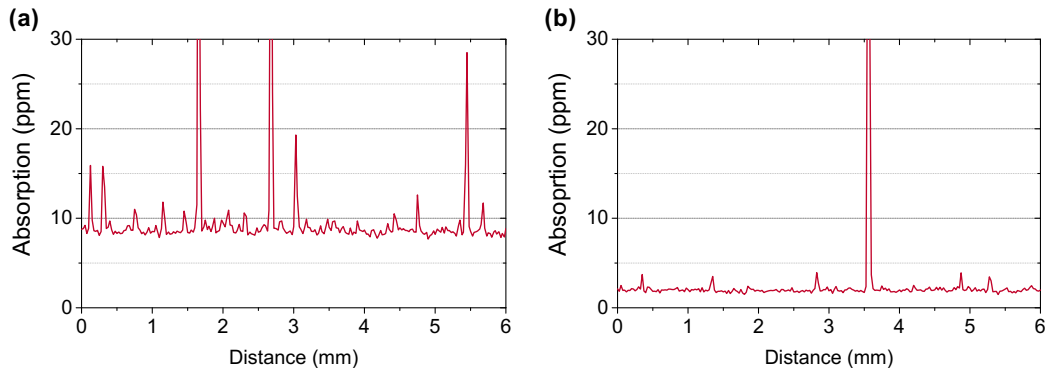

Figure 6. PCI absorption z-scan of the ZrO_2/SiO_2 RF sputtered coating from (a) an as-deposited sample and (b) the same sample annealed at 300°C for 24 hours in air.

Table 3 gives the baseline absorption of the test coatings that were subject to post-deposition annealing. Both before and after post-deposition annealing baseline PCI absorption and LIDT are given for comparison. The results show a consistent reduction in baseline absorption after annealing. However, this improvement in absorption does not directly translate into LIDT.

Table 3. Comparison of baseline PCI absorption and LIDT before and after post-deposition annealing at 300°C in air for 24 hours for coating samples 1, 2 and 4 (see table 2).

#	Coating	Before annealing		After annealing	
		α (ppm)	LIDT (J/cm^2)	α (ppm)	LIDT (J/cm^2)
1	ZrO_2/SiO_2 RF sputter	9.1	74	2.1	46
2	Ta_2O_5/SiO_2 RF sputter	2.9	48	1.9	41
4	TiO_2/SiO_2 ebeam/thermal	24.7	8	14.9	15

The differences in LIDT are heavily dependent on the failure mechanism, either in terms of failure of the coating or the substrate. Where there is no improvement in LIDT after annealing, the substrate had already failed at a lower damage threshold and no further improvement was likely. From figure 6 (a), it should be noted that considerable variation in the absorption across the sample surface may indicate a significant content of inclusions or microstructure which could contribute heavily to the observed LIDT, and the related mechanisms discussed in detail in the Wood *et al.* and Lowdermilk *et al.* [5,6].
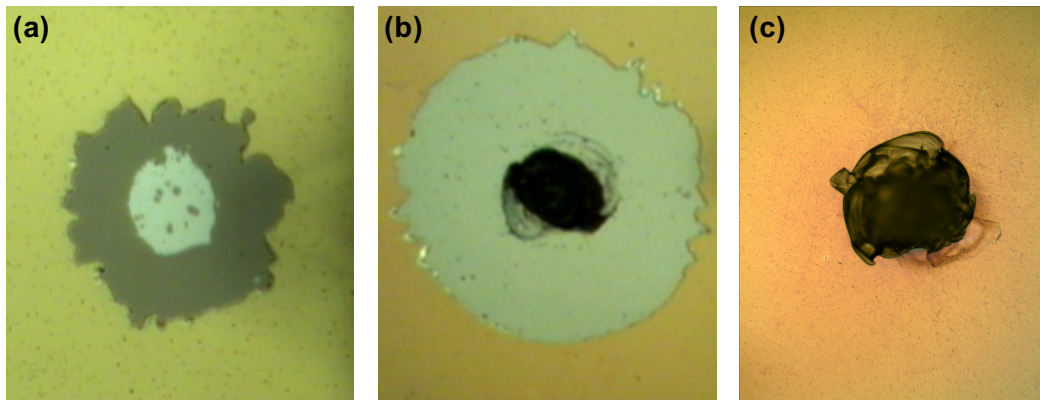

Figure 7. Optical microscope images highlighting the damage morphology of a damage pit from the (a) Nb_2O_5/SiO_2 RF sputtered, (b) ZrO_2/SiO_2 RF sputtered and (c) ZrO_2/SiN DC sputtered coatings.

LIDT damage types include material only ablation (seen in the Nb_2O_5/SiO_2 RF sputtered coating, figure 7 (a)), coating loss and substrate damage (seen in the such as the ZrO_2/SiO_2 RF sputtered (figure 7 (b)) and substrate only damage such as (seen in the such as the ZrO_2/SiN DC sputtered coating (figure 7 (c)). In some ebeam coating sample cases thermally induced local damage was also observed.

Atomic force microscopy (AFM) measurements were also made on a Veeco Dimension V AFM/Nanomechanical Tester. The AFM was set to run in contact mode with a 0.4 – 0.7 µm thick non-conductive silicon nitride tip, and is typically able to measure height differences ranging from sub-nanometer to a few microns. Figure 8. reiterates the results of the optical micrographs and shows extensive subsurface damage and substrate failure. Surface roughness, R, of the undamaged coating regions were also measured, and gave R = 11.1 ± 0.6 nm for the ZrO_2/SiO_2 coating and R = 0.85 ± 0.07 nm for the Nb_2O_5/SiO_2 coating.
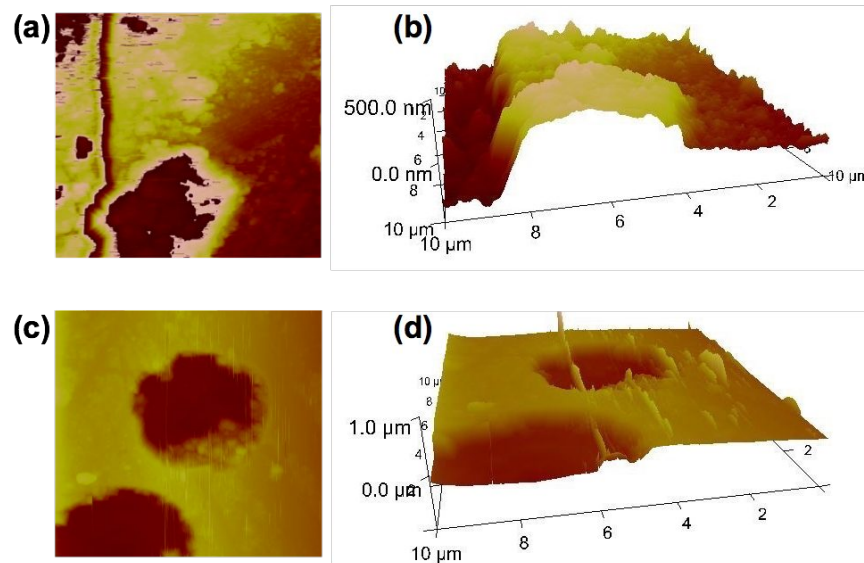
Figure 8. AFM scans in 2D and 3D for the (a) and (b) RF sputtered ZrO_2/SiO_2 and (c) and (d) ebeam deposited Nb_2O_5/SiO_2 coating.

6. CONCLUSIONS

It can be shown that a post-deposition annealing at 300ºC consistently reduces absorption as measured by PCI but does not significantly increase the LIDT. In the case of the ZrO_2/SiO_2 coating, the LIDT is largely limited by the substrate properties: upheld by both substrate PCI measurements and the substrate failure of the top performing samples. There are many possible reasons for this lack of LIDT improvement including that the baseline absorption is not the dominant mechanism at the measured levels, instead e.g. electric field breakdown effects may be more prevalent. Similarly, the micro-inclusion content and nanostructure may also be critical and this could help explain the observed improvement in RF sputtered materials over their namesakes grown by electron beam evaporation; this can often be seen by surface roughness or by surface scan PCI.

ZrO_2 appears to have great promise, offering good LIDT performance when used with either SiO_2 or SiN despite also having high absorption in the latter case - perhaps exhibiting non-linear properties at high optical fluence. It was expected that the nitride would have a higher damage threshold due to the higher thermal conductivity [7], which may be the case, but instead it appears limited by the substrate for these samples.

The surface variability in absorption offers deposition technique related clues that point to the need for higher chamber cleanliness, better control of inclusions (longer source conditioning, better source cleaning, lower deposition rates, longer source-to-substrate separation, *etc*), and may also require better substrate cleaning and handling.

From the range of PCI absorption measurements collected for the uncoated substrates (a factor of 400 for seemingly identical transmission by spectrophotometry), observed enhancement of scratches after laser damage testing on some samples, and an apparent threshold ceiling prior to substrate failure; it would seem prudent to ensure a more standardized starting point for future substrate selection based not only on internal losses but also surface finish, for which such a correlation has long been reported [8]. Future work would therefore include before and after laser damage microscale surface analysis.

A deeper study would also look closely at a wider collection of deposition materials, including HfO_2, Al_2O_3 and other oxides commonly used in high fluence applications, and in addition the coating design for aspects of electrical field optimization, including potentially a mixed material / graded refractive index pulsed DC sputtered ZrO_2/SiN.

Further investigations intend to explore alternative starting materials for the same final coating chemistry for reactive ebeam, such as Nb_2O_5 from Nb metal and SiO_2 from Si to reduce inclusions and scatter centers. A study of the effect of the sputtering rate of ZrO_2 on the intrinsic properties and any resultant change in LIDT would also be desirable, given the demonstrated promising performance of the material.

ACKNOWLEDGEMENTS

REFERENCES

[1] Furukawa, Y., Kitamura, K., Alexandrovski, A., Route, R. K., Fejer, M. M. and Foulon, G., "Green-induced infrared absorption in MgO doped LiNbO3," Appl. Phys. Lett. 78, 1970-1972 (2001).

[2] Alexandrovski, A., Fejer, M. , Markosyan, A. and Route, R., "Photothermal common-path interferometry (PCI): new developments," Proc. SPIE 7193, 71930D 1-13 (2009).

[3] Markosyan, A. S. , Route, R., Fejer, M. M., Patel, D. and Menoni, C. S., "Spontaneous and induced absorption in amorphous Ta_2O_5 dielectric thin films," Proc. SPIE 8190, 81900F (2011).

[4] Hass, G., "Preparation, properties and optical applications of thin films of titanium dioxide," Vacuum 2(4), 331-345 (1952).

[5] Wood, R.M., Taylor, R.T., Rouse, R.L., "Laser damage in optical materials at 1.06 μm," Opt. and Laser Technol. 7(3), 105-111 (1975).

[6] Lowdermilk, W. H. and Milam, D., "Laser-induced surface and coating damage," IEEE J. Quantum Elect., Vol 17(9), 1888-1903 (1981).

[7] Guenther, A. H. and McIver, J. K., "The role of thermal conductivity in the pulsed laser damage sensitivity of optical thin films," Thin Solid Films 163, 203-214 (1988).

[8] House, R. A., Bettis, J. R., Guenther, A.H., "Correlation of laser-induced damage threshold with surface structure and preparation techniques of several optical glasses at 1.06 μm," NBS Special Publication 435, 305-320 (1975).